Pairing, ferromagnetism, and condensation of a normal spin-1 Bose gas

Stefan S. Natu and Erich J. Mueller

Phys. Rev. A **84**, 053625 — Published 22 November 2011

DOI: 10.1103/PhysRevA.84.053625

Pairing, Ferromagnetism, and Condensation of a normal spin-1 Bose gas

Stefan S. Natu* and Erich J. Mueller
Laboratory of Atomic and Solid State Physics, Cornell University, Ithaca, New York 14853, USA.

We find the conditions under which the normal state of a spin-1 Bose gas is unstable towards condensation, ferromagnetism, liquid crystalline-like nematicity and Bardeen-Cooper-Schrieffer-like pairing. When the spin-dependent interactions are much weaker than the density-density interaction there is direct transition from a featureless normal state to a fully ordered Bose-Einstein condensate with either ferromagnetic or nematic order. When the spin independent and dependent interactions are of comparable magnitude, we find several different symmetry breaking transitions at intermediate temperatures *above* the Bose-condensation transition temperature. We make predictions for the T_c for these transitions, and assess the role of magnetic field and finite system size.

I. INTRODUCTION

The interplay of superconductivity/superfluidity and magnetism is fundamental [1]. Theoretical and experimental studies of Bose gases with internal degrees of freedom have begun to explore this physics, elucidating the subtle connections between Bose condensation of single particles (BEC) and competing/complementary orders such as pair condensation, ferromagnetism, and liquid-crystal like nematicity [2–7]. Most of the exciting work on this rich system has focussed on the regime where the interactions are nearly spin independent. There superfluidity *complements* rather than competes with other orders, and the finite temperature phase diagram is very simple: as the temperature is lowered, a featureless normal state transitions into a fully ordered Bose condensate, where symmetries associated with the spin and charge degrees of freedom are simultaneously broken. The focus of this paper is the regime where spin dependent and spin independent interactions are of comparable magnitude allowing the existence of "less-ordered" phases: ferromagnetism without condensation, and a bosonic analog of Cooper pairs.

In spinless bosons, paired states are almost always unstable towards mechanical collapse: the same attraction which creates pairs leads to a negative compressibility [8, 9]. In the spin-1 Bose gas the BCS instability occurs when "repulsive" spin dependent and spin-independent interactions lead to an effective "attractive" interaction in the spin singlet channel. Repulsive interactions in the spin-2 channel prevent collapse. Somewhat counterintuitively, in this context the paired state is less ordered than a single-particle condensate.

In this paper we use a Random Phase Approximation (RPA-X), which includes exchange to study the instabilities of the normal state towards ferromagnetism, nematicity and pairing. This paper is organized as follows: In Section II we present a discussion of the Hamiltonian of the spin-1 gas, and the possible ordered states that may be present. In Section III we outline the formalism of the RPA-X, and calculate the ferromagnetic and pair susceptibilities for the interacting Bose gas in terms of the susceptibilities of the non-interacting gas. In Section IV we present the results of our calculation, and plot the instability lines with and without magnetic field for different values of the spin-dependent interaction strength. Finally we discuss finite size effects, and the possibility of experimentally observing this phase diagram.

II. HAMILTONIAN AND POSSIBLE ORDERS

The Hamiltonian of a spin-1 Bose gas is the sum of a kinetic and interaction term, $H = \mathcal{H}_{kin} + \mathcal{H}_{int}$. In the presence of a magnetic field in the $\hat{z}$ direction, the kinetic term has the form $\mathcal{H}_{kin} = \sum_{k\sigma} \epsilon_{k\sigma} a^\dagger_{k\sigma} a_{k\sigma}$, where $a_{k\sigma}$ is the annihilation operator for a boson with momentum k and spin projection $\sigma = -1, 0, 1$. The dispersion is $\epsilon_{k0} = k^2/2m - \mu$, $\epsilon_{k\pm1} = k^2/2m - \mu + q \pm p$, where p/q are linear/quadratic in the magnetic field. There is no spin-orbit coupling, allowing us to eliminate the linear Zeeman effect (p) by working in a rotating frame. Henceforth, we set $p = 0$. The quadratic Zeeman field produces a magnetic anisotropy which can be experimentally tuned [10]. Assuming short range interactions, symmetry forces the interaction Hamiltonian to be [3, 4]:

$$\mathcal{H}_{int} = \frac{1}{2}\int d\mathbf{r}\ \psi^\dagger_\alpha \psi^\dagger_\beta \psi_\gamma \psi_\delta (c_0 \delta_{\alpha\delta}\delta_{\beta\gamma} + c_2 \mathbf{S}_{\alpha\delta}\cdot\mathbf{S}_{\beta\gamma}), \quad (1)$$

where the greek indices denote the spin projection and $\psi_\sigma(r) = \frac{1}{V}\sum_k e^{ikr} a_{k\sigma}$ is the the boson field operator.

The two coupling constants, c_0 and c_2 represent spin independent and spin dependent interactions and $\mathbf{S}$ is the vector $\{S^x, S^y, S^z\}$ where S^i are 3×3, spin-1 matrices. The interactions are expressed in terms of the microscopic scattering lengths in the spin-0 (a_0) and spin-2 (a_2) channels and atomic mass m as: $c_0 = 4\pi(a_0 + 2a_2)/3m$ and $c_2 = 4\pi(a_2 - a_0)/3m$.

The spin-1 gas can present several types of order, summarized in Table I where we use the shorthand $\hat{S}^i = S^i_{\alpha\beta}\psi^\dagger_\alpha\psi_\beta$ and $\hat{S}^i\hat{S}^j = (S^i\cdot S^j)_{\alpha\beta}\psi^\dagger_\alpha\psi_\beta$. Single particle condensate order (**C**) is always accompanied by either ferromagnetic (**FC**) or nematic order (**NC**). Mean field examples of these condensed states are $|FC\rangle =$

*Electronic address: ssn8@cornell.edu

TABLE I: Orders in spin-1 gas.

Order	Symbol	Order Parameter
ferromagnetic	**F**	$\langle \hat{S}^i \rangle \neq 0$
nematic	**N**	$\langle \hat{S}^i \hat{S}^j \rangle \neq \delta_{\mu\nu}$
single particle (BEC)	**C**	$\langle \psi_\mu \rangle \neq 0$
pair	**P**	$\sum_k \langle a^\dagger_{\mu\mathbf{k}} a^\dagger_{\nu\text{-}\mathbf{k}} \rangle \neq 0$

$(\psi_1^\dagger)^N|0\rangle$, and $|NC\rangle = (\psi_0^\dagger)^N|0\rangle$, with the former seen in ^{87}Rb, and the latter in ^{23}Na. The singlet state from [11] with all particles in $k = 0$, $|S\rangle = ((a^\dagger_{0,\mathbf{k=0}})^2 - 2a^\dagger_{1,\mathbf{k=0}}a^\dagger_{-1,\mathbf{k=0}})^{N/2}|0\rangle$, has off-diagonal single-particle order [ie. $\lim_{|r-r'|\to\infty}\langle\psi_0^\dagger(r)\psi_0(r')\rangle \neq 0$] and in the thermodynamic limit should be considered as an **NC** state [12]. An example of a paired, **P**, state would be a condensate of singlet pairs $|P\rangle = \kappa^{N/2}|0\rangle$, where $\kappa = \sum_k \left(a^\dagger_{0\mathbf{k}}a^\dagger_{0\text{-}\mathbf{k}} - 2a^\dagger_{1\mathbf{k}}a^\dagger_{-1-\mathbf{k}}\right)$. Unlike $|S\rangle$, the state $|P\rangle$ has no off-diagonal single particle order.

Although the 2D phase diagram is well established [13–15], contradictory results have appeared regarding the nature of ferromagnetism in the 3D phase diagram. Both Kun Yang [15], and Gu and Klemm [16] erroneously found that arbitrarily weak *attractive* spin-dependent interactions ($c_2 < 0$) drive a ferromagnetic instability with $T_c^F > T_{BEC}$. Kis-Szabó, Széfalusy and Szirmai [17] more accurately modeled the role of "quantum statistics" in the normal state of the spin-1 gas, and found a finite threshold for this instability.

The central physics is that due to quantum statistics, two bosons in the same spin state have an enhanced probability of being close to one another. As a consequence of these "exchange correlations", repulsive spin-independent interactions ($c_0 > 0$) suppress spin ordering. It is only when $|c_2| \gtrsim c_0$ that the intrinsic spin-independent interactions can overcome these exchange forces, and lead to ferromagnetism. It was precisely this exchange physics that was excluded in [15, 16].

III. FORMALISM

A. Overview

We calculate the instabilities of the normal state using a Hartree-Fock Random Phase Approximation (RPA-X) in which all direct (bubble) and exchange (ladder) graphs are summed. This is a self-consistent approximation which accurately describes the dilute limit of a gas of particles with short-range interactions ($na^3 \ll 1$, where a is the scattering length in a given channel). Most cold-atom experiments are in the dilute regime. In 3D, we expect more sophisticated theories to yield only small quantitative corrections to our results, while leaving unaffected our qualitative conclusions [18, 19]. The RPA-X can be derived from linear response of the Hartree Fock approximation [8].

We calculate the density-density, longitudinal (χ_z) and transverse spin ($\chi_\pm$) and pairing (Π) susceptibilities of the homogeneous interacting spinor Bose gas. A divergence of the zero frequency, long wavelength susceptibility, $\chi^{-1}(\mathbf{k} = 0, \omega = 0) = 0$ signals an instability in that channel.

B. Definitions

The relevant response functions are

$$\chi^{\gamma\delta}_{\alpha\beta\mathbf{p}}(t) = \frac{1}{i}\langle\sum_{k,q} a^\dagger_{\delta\mathbf{k}}(t)a_{\gamma\mathbf{k+p}}(t)a^\dagger_{\beta\mathbf{q}}(0)a_{\alpha\mathbf{q-p}}(0)\rangle \quad (2)$$

$$\Pi^{\gamma\delta}_{\alpha\beta\mathbf{p}} = \frac{1}{i}\langle\sum_{k,q} a^\dagger_{\delta\mathbf{k}}(t)a^\dagger_{\gamma\mathbf{p-k}}(t)a_{\beta\mathbf{q}}(0)a_{\alpha\mathbf{p-q}}(0)\rangle \quad (3)$$

where $t > 0$, and the greek subscripts denote spin indices and $\mathbf{p}$ is the momentum [20, 21]. The longitudinal and transverse spin correlation functions are

$$\chi_{z\mathbf{p}}(t) = -i\langle\hat{S}^z_{\mathbf{p}}(t)\hat{S}^z_{-\mathbf{p}}(0)\rangle = -\sum_{\alpha,\delta}(-1)^{\alpha\delta}\chi^{\delta\delta}_{\alpha\alpha\mathbf{p}}(t) \quad (4)$$

and

$$\chi_\pm = -i\langle\hat{S}^+_{\mathbf{p}}(t)\hat{S}^-_{-\mathbf{p}}(0)\rangle = \chi^{10}_{01}+\chi^{0\ 1}_{0\ -1}+\chi^{-1\ 0}_{0\ -1}+\chi^{-10}_{\ 10} \quad (5)$$

where $\alpha, \delta \in \{1, -1\}$, $\hat{S}^i_{\mathbf{p}}(t) = \sum_{\mathbf{q}} a^\dagger_{\mathbf{p+q}/2}(t)S^i a_{\mathbf{p-q}/2}(t)$, and $\mu = \{z, \pm\}$.

C. Expressions for responses

In the RPA-X, the susceptibility of the interacting gas is

$$(\chi^{RPA})^{\gamma\eta}_{\alpha\beta} = (\chi^0)^{\gamma\eta}_{\alpha\beta}\delta_{\alpha\eta}\delta_{\beta\gamma} + \sum_{\mu\nu}(\chi^0)^{\gamma\eta}_{\eta\gamma}\mathbf{V}^{\gamma\eta}_{\mu\nu}(\chi^{RPA})^{\nu\mu}_{\alpha\beta} \quad (6)$$

$$(\Pi^{RPA})^{\gamma\eta}_{\alpha\beta} = (\Pi^0)^{\gamma\eta}_{\alpha\beta}\delta_{\alpha\eta}\delta_{\beta\gamma} + \sum_{\mu\nu}(\Pi^0)^{\gamma\eta}_{\eta\gamma}\mathbf{V}^{\gamma\eta}_{\mu\nu}(\Pi^{RPA})^{\mu\nu}_{\gamma\eta} \quad (7)$$

The effective interaction potential $V^{\gamma\eta}_{\mu\nu}$ of Eq. (1), which includes both direct and exchange graphs, is explicitly given in Appendix A.

D. Free response functions

The non-interacting Green's functions are diagonal in spin space: $(\chi^0)^{\gamma\eta}_{\alpha\beta\mathbf{p}}(t) = 0$, and $(\Pi^0)^{\gamma\eta}_{\alpha\beta\mathbf{p}}(t) = 0$ unless $\eta = \alpha$ and $\gamma = \beta$,

$$(\chi^0)^{\beta\alpha}_{\alpha\beta}(p,\omega) = \int \frac{d^3\mathbf{k}}{(2\pi)^3}\frac{n(\epsilon_{k,\alpha}) - n(\epsilon_{k+p,\beta})}{\omega - (\epsilon_{k+p\beta} - \epsilon_{k\alpha})} \quad (8)$$

$$(\Pi^0)^{\alpha\beta}_{\beta\alpha}(\mathbf{p},\omega) = \int \frac{d^3\mathbf{k}}{(2\pi)^3}\frac{n(\epsilon_{\mathbf{k},\alpha}) + n(\epsilon_{\mathbf{k+p},\beta})}{\omega - (\epsilon_{\mathbf{k+p}\beta} + \epsilon_{\mathbf{k}\alpha})} \quad (9)$$

Here $n(\epsilon_{k\sigma}) = (e^{\beta\epsilon_{k\sigma}} - 1)^{-1}$ is the Bose-Einstein distribution at temperature $T = 1/\beta$. For a non-interacting gas, the spin susceptibility χ^0, pairing susceptibility Π^0 and compressibility all diverge as $\mu \to 0$ from below, marking single particle condensation. In the absence of the quadratic Zeeman shift ($q = 0$), the T_c for this transition is given by the familiar formula $k_B T_{BEC} = \frac{2\pi}{m}(\frac{n}{3\zeta(3/2)})^{2/3}$.

At $k = 0$ and $\omega = 0$, these non-interacting response functions may be written in terms of the polylogarithm functions $g_\nu(z) = \sum_j z^j/j^\nu$:

$$\chi_{-1\ 1}^{1-1}(0,0) = -\frac{m}{2\pi\Lambda_T} g_{1/2}(e^{\beta(\mu-q)}) \tag{10}$$

$$(\chi^0)_{01}^{10}(0,0) = \frac{m}{4\pi\Lambda_T}(T/q)[g_{3/2}(e^{\beta(\mu-q)}) - g_{3/2}(e^{\beta\mu})]$$

$$\Pi_{\alpha\beta}^{\beta\alpha}(0,0) = -\frac{m}{\pi\Lambda_T} g_{1/2}(e^{\beta\mu_{\rm eff}})$$

where $\mu_{\rm eff} = \mu - q$ for $\alpha = \pm 1$ and $\beta = \mp 1$, and $\mu_{\rm eff} = \mu$ for $\alpha = \beta = 0$. The thermal wavelength is $\Lambda_T = \sqrt{2\pi/mk_BT}$.

IV. RPA RESPONSE FUNCTIONS

In Appendix B we show that the ferromagnetic response functions are:

$$\chi_z^{RPA}(\mathbf{k},0) = \frac{2(\chi^0)_{-1\ 1}^{1-1}(\mathbf{k},\omega)}{1-(c_0+3c_2)(\chi^0)_{-1\ 1}^{1-1}(\mathbf{k},0)} \tag{11}$$

$$\chi_\pm^{RPA}(\mathbf{k},0) = \frac{2(\chi^0)_{10}^{10}(\mathbf{k},0)}{1-(c_0+3c_2)(\chi^0)_{01}^{10}(\mathbf{k},0)} \tag{12}$$

In Appendix C we calculate the response to pairing. To detect pairing, it suffices to consider the singlet pairing susceptibility, $\Theta = (\Pi_{00}^{00} - 2\Pi_{-1\ 1}^{1-1})^{RPA}$,

$$\Theta = \frac{\Pi^+ - 2\Pi^0 + \Pi^0\Pi^+(c_0-2c_2)}{1-(c_0-c_2)\Pi^+ - c_0\Pi^0 + (c_0-c_2)(c_0+c_2)\Pi^+\Pi^0}.$$

with $\Pi^0 \equiv (\Pi^0)_{00}^{00}$ and $\Pi^+ \equiv (\Pi^0)_{-1\ 1}^{1-1}$. When $q = 0$ $(\Pi^0)_{00}^{00} = (\Pi^0)_{-1\ 1}^{1-1} = (\Pi)^0$, and we get $\Theta^{-1} \propto 1 - (c_0 - 2c_2)(\Pi)^0$.

V. RESULTS

A. Mechanical stability

We address the mechanical stability of the gas by looking for a divergence in the RPA density-density response function. The density-density response function is obtained by taking the Trace of χ^{RPA} in (Eq. 8), which is found to be proportional to $(1 - 2(2c_0 + c_2)\chi^0)^{-1}$, where χ^0 is the non-interacting response function. Writing c_0 and c_2 in terms of the scattering lengths in the spin-0 and spin-2 channels we find, $2c_0 + c_2 \propto a_0 + 5a_2$. Therefore is a positive scattering length in the spin-2 channel is crucial for the stability of the cloud.

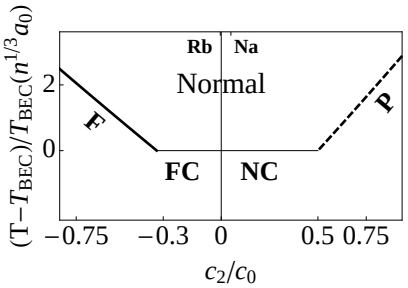

FIG. 1: **Instabilities of the Normal state within the RPA-X**: Thick solid/dashed lines are the ferromagnetic and pairing transition temperatures measured from the ideal Bose gas transition and scaled by $n^{1/3}a_0$ as a function of spin-dependent interaction c_2. Thin solid line is the T_c for Bose condensation in an ideal gas (ferromagnetic or polar depending on the sign of c_2). For $c_2 > 0.5c_0$, the normal state is unstable to a rotationally symmetric paired singlet phase (P) with a $T_c > T_{BEC}$. For $c_2 < -c_0/3$, the normal state becomes unstable to a ferromagnet (F). At some lower temperature, we expect a transition from the F state to a FC and from the paired state (P) to a nematic condensate (NC). However these cannot be calculated by looking at the instabilities of the normal state. Tick marks on the top axis show typical scattering lengths for ^{87}Rb and ^{23}Na.

B. Stability against ferromagnetism and pairing

Next we consider the instabilities towards ferromagnetism and pairing. Within Hartree-Fock, c_0 stabilizes the normal state against ferromagnetism. The interaction term $\langle H_{int}\rangle = c_0(n^2 + \sum_{\mu\nu}\langle\psi_\mu^\dagger\psi_\nu\rangle\langle\psi_\nu^\dagger\psi_\mu\rangle)$ is smallest in the absence of any spin order: $\langle\psi_\mu^\dagger\psi_\nu\rangle = \delta_{\mu\nu}n/3$. The opposite occurs in fermions where this exchange term is negative, producing an attraction between like spins, giving rise to the Stoner instability [22].

From Eq. 11, and the fact that $\chi^0(0,0) < 0$ we see that the spin susceptibility only diverges when $c_2 < 0$ with $|c_2| > c_0/3$. Similarly, at $q = 0$, the pairing susceptibility only diverges when $c_2 > 0$ with $c_2 > c_0/2$. Writing c_0 and c_2 in terms of the spin-0 and spin-2 scattering lengths, we see that the pairing instability occurs whenever a_0 is negative. This is reminiscent of the Cooper instability in fermions, where arbitrarily weak attraction leads to a superconducting transition. Furthermore as shown above, as long as a_2 is positive, the gas is expected to be mechanically stable. This makes the spin-1 gas one of

the simplest examples of a system where a stable bosonic analog of BCS pairing is supported.

For weak interactions ($|c_2 n| \ll k_B T$), these instabilities occur near $\mu = 0$. Expanding the susceptibilities for small μ at $q = 0$ gives to leading order:

$$t_{\rm mag} = \frac{T_c^{\rm mag} - T_{\rm BEC}}{T_{\rm BEC}} = 4.84\left(\frac{1}{3} - \frac{c_2}{c_0}\right) n^{1/3} a_0 \quad (13)$$

$$t_{\rm pair} = \frac{T_c^{\rm pair} - T_{\rm BEC}}{T_{\rm BEC}} = 6.44\left(\frac{c_2}{c_0} - \frac{1}{2}\right) n^{1/3} a_0.$$

The instability lines at $q = 0$ are plotted in Fig. 1.

C. Role of finite magnetic field

We now explore the role of the quadratic Zeeman effect: $q < 0$ favors magnetism in the $\pm\hat{z}$ direction ($\mathbf{F}_\parallel$ – Ising order – signalled by diverging χ_z), and pairs in the $m_F = \pm 1$ states ($\mathbf{NP}_\perp$: $|\langle\psi_1^\dagger\psi_{-1}^\dagger\rangle| > |\langle\psi_0^\dagger\psi_0^\dagger\rangle|$); while $q > 0$ favors magnetism in the $\mathbf{x}-\mathbf{y}$ plane ($\mathbf{F}_\perp$ – x-y order – diverging $\chi_\pm$), and $m_F = 0$ pairs ($\mathbf{NP}_\parallel$: $|\langle\psi_0^\dagger\psi_0^\dagger\rangle| > |\langle\psi_1^\dagger\psi_{-1}^\dagger\rangle|$). Finite q also shifts the BEC transition temperature: the density is given by $n\Lambda_T^3 = g_{3/2}(e^{\beta\mu}) + 2g_{3/2}(e^{\beta(\mu-q)})$, with condensation at $\mu = q$ for $q < 0$ and at $\mu = 0$ for $q > 0$. For small q one finds $T_{\rm BEC}^{q\neq 0} = T_{\rm BEC}^{q=0} + \xi\sqrt{T_{\rm BEC}^{q=0} q}$ with $\xi = 0.3$ for $q < 0$ and $\xi = 0.6$ for $q > 0$.

Figure 2(a) illustrates the instabilities of the normal state for $c_2 < 0$, where the only relevant instabilities are ferromagnetism and single particle condensation. For $q < 0$ and $|c_2| > c_0/3$ an Ising ferromagnetic instability always precedes condensation. For $q > 0$ there is a threshold q below which $\mathbf{x}-\mathbf{y}$ ferromagnetism precedes condensation. The dependance of this threshold on c_2 is shown in Figure 2(b). For c_2 near $-c_0/3$, one finds: $q_c = T_{\rm BEC}^{q=0}(10.6(a_0 n)^{1/3}\alpha)^2$, where $\alpha = 1/3 - |a_2|/a_0$.

Figure 3(a) illustrates the instability lines for $c_2 > 0$, where the only relevant instabilities are pairing and single particle condensation. Finite q enhances single particle condensation, and for a given q, there is a threshold value of c_2 required to find a pairing instability as shown in Fig.3(c).

D. Instability to nematicity

In the spin-1 gas, there is no normal "nematic" phase. The reason for this is that the interaction Hamiltonian does not contain a term $\propto \langle\hat{S}_\mu\hat{S}_\nu\rangle^2$ following the conventions of Table. I. Thus the appearance of nematic order must be associated with simultaneous single-particle or pair order.

The quadratic Zeeman effect couples to spin fluctuations ($\propto \langle\hat{S}_z^2\rangle$), and explicitly breaks the symmetry in spin space. For $q > 0$, the $m_F = 0$ state is lower in energy and has a higher density than the $m_F = \pm 1$ states

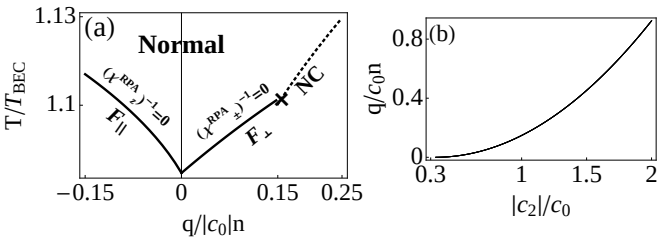

FIG. 2: **Instability with $\mathbf{c_2 < 0}$**: (a): Instabilities of the unordered normal state with $c_2 = -c_0$ as a function of q. Solid curves give the T_c for a non-condensed ferromagnetic gas, normalized to $T_{BEC}|_{q=0}$ (defined in Fig.1 caption). At some lower temperature, one expects a transition to a ferromagnetic condensate (**FC**). For $q < 0$, this T_c always exceeds the ideal Bose gas transition temperature. For $q > 0$, the ideal gas temperature meets the T_c for ferromagnetism at some finite q (marked by $\times$). Beyond this point, the normal state is unstable to forming a nematic condensate. (b): Location of $\times$ as a function of interaction strength.

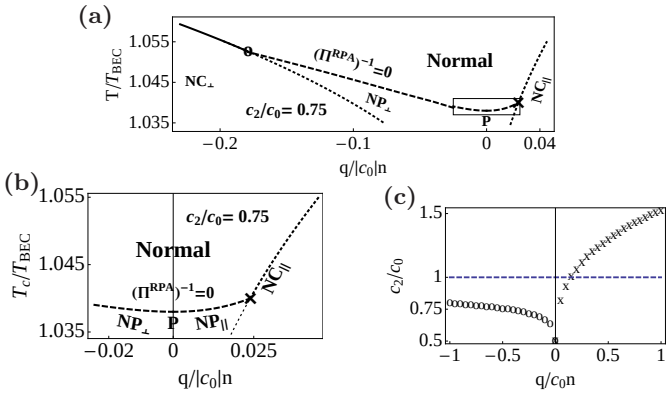

FIG. 3: **Instabilities with $\mathbf{c_2 > 0}$**: (a): Instabilities of the unordered state with $c_2 = 0.75c_0$. At large negative q, the normal state is unstable towards a single-particle condensate ($\mathbf{NC}_\perp$) with a spinor order parameter $\zeta = \{e^{i\phi}, 0, 1\}$), with arbitrary ϕ. For $-|q_{c1}|(\times) < q < |q_{c2}|(o)$ the instability is towards pairing. At $q = 0$ the paired phase is a spin singlet with no spin fluctuations. For $q \neq 0$, the paired phase has spin fluctuations in the $\mathbf{x}-\mathbf{y}$ plane. For large $q > 0$, the normal state is unstable towards a polar condensate with spinor $\zeta = \{0, 1, 0\}$. Dotted lines are the ideal gas condensation T_c as a function of q. (b): Details of dashed rectangle in (a), showing instabilities towards pairing. (c): Critical values of q at which pair instability gives way to single particle instability (*i.e.* locations of $\times$ and o) for different interaction strengths.

and vice-versa for $q < 0$. Similarly for $q > 0$ the magnitude of the pair order parameter: $|\langle\psi_1^\dagger\psi_{-1}^\dagger\rangle| < |\langle\psi_0^\dagger\psi_0^\dagger\rangle|$, while the reverse is true for $q < 0$.

VI. FINITE SIZE EFFECTS

We can estimate the role of finite size effects by looking at the instabilities at finite $k = 2\pi/L$ (rather than at $k = 0$), where L is the size of the cloud. These finite size effects are crucial in the scalar gas with attractive

interactions, where there is no Bose-Einstein condensation in the thermodynamic limit [8]. Here we find only small corrections to location of the threshold value of $|c_2|/c_0$. To leading order in $k\Lambda_T \ll 1$, the threshold for ferromagnetism is $a_2/a_0 = -\frac{1}{3} - k\Lambda_T^2/(12\pi^2 a_0)$, while the threshold for pairing is $a_2/a_0 = \frac{1}{2} + k\Lambda_T^2/(8\pi^2 a_0)$. These shifts are no greater than 10% for a system of size $L \sim 100\mu$m, typical in cold-atom experiments.

VII. OBSERVABILITY

A few comments are in order about the experimental observability of this phase diagram. Thus far all experiments on spin-1 gases have used ^{87}Rb and ^{23}Na which have extremely weak spin dependent interactions. The scattering lengths could be enhanced by using microwave induced Feshbach resonances [23]. Alternatively, superexchange a lattice can generate strong nearest neighbor anti-ferromagnetic interactions (effectively large c_2) [24]. Moreover ^{7}Li and ^{39}K are currently believed to have large negative c_2, and thus are promising candidates for observing a ferromagnetic normal state [25, 26].

A number of probes can be used to distinguish the nematic phases, detect pairing and identify ferromagnetism. These include optical birefringence [27], momentum distributions via time-of-flight, noise correlations [28], and the nature of vortices [5].

VIII. CONCLUSIONS

Competing orders lie at the heart of modern condensed matter physics. For a Bose gas with internal degrees of freedom, the competition between spin and charge physics produces a rich finite temperature phase diagram with superfluid, ferromagnetic, nematic and paired phases. For weak spin dependent interactions, bosonic exchange stabilizes a fully disordered normal state against any spin ordering. For strong attractive spin dependent interactions, spin ordered phases are present in the absence of superfluidity. Furthermore for strong repulsive spin-dependent interactions, we find a spin-singlet paired phase, analogous to a BCS superconductor. We expect to see similar physics in higher spin bosonic gases where a normal nematic, or quintet (spin-2) pairing may occur in addition to the phases described here.

IX. ACKNOWLEDGEMENTS

We thank Stefan K. Baur, Mukund Vengalattore, Joel E. Moore, Xiaoling Cui, and Ari Turner for useful conversations. This material is based upon work supported by the National Science Foundation through grant No. PHY-0758104.

Appendix A: Analytic structure of non-interacting response functions

In this Appendix, we develop the analytic structure of $\chi^{0\beta\alpha}_{\alpha\beta}$ defined as:

$$(\chi^0)^{\beta\alpha}_{\alpha\beta}(p,\omega) = \int \frac{d^3\mathbf{k}}{(2\pi)^3} \frac{n(\epsilon_{k,\alpha}) - n(\epsilon_{k+p,\beta})}{\omega - (\epsilon_{k+p\beta} - \epsilon_{k\alpha})} \qquad \text{(A-1)}$$

where the greek indices are used to represent the hyperfine spin levels $m_F = 0, \pm 1$. Diagramatically this can be represented by a bubble graph where a particle (with spin-α) and hole (with spin-β) pair is created. This tensor has the property that: $(\chi^0)^{1\alpha}_{\alpha 1} = (\chi^0)^{-1\alpha}_{\alpha -1}$ and $(\chi^0)^{\alpha 1}_{1\alpha} = (\chi^0)^{\alpha -1}_{-1\alpha}$ for any α, because the quadratic Zeeman shift does not distinguish between the $m_F = \pm 1$ states. Furthermore $(\chi^0)^{0\alpha}_{\alpha 0} = (\chi^0)^{\alpha 0}_{0\alpha}$ for any α.

For $q = 0$, all the spin states are identical, and we can set $(\chi^0)^{\beta\alpha}_{\alpha\beta}(p,\omega) = \chi(p,\omega) = \int \frac{d^3\mathbf{k}}{(2\pi)^3} \frac{n(\epsilon_k) - n(\epsilon_{k+p})}{\omega - (\epsilon_{k+p} - \epsilon_k)}$, whose structure has been thoroughly explored in [8]. At long wave-lengths $p\Lambda_T \ll 1$:

$$\chi(\mathbf{p},0) = -\frac{m}{2\pi\lambda_T}\left(g_{1/2}(e^{\beta\mu}) - \sqrt{|\pi/(\beta\mu)|} + \frac{i\pi}{p\Lambda_T} \log\left(\frac{\sqrt{\beta\mu} - \frac{p\Lambda_T}{4\sqrt{\pi}}}{\sqrt{\beta\mu} + \frac{p\Lambda_T}{4\sqrt{\pi}}} \right) \right) \qquad \text{(A-2)}$$

where $g_\nu(z)$ is the polylogarithm function. For $q \neq 0$, first note that $\chi^{\beta\alpha}_{\alpha\beta}(0,0) = \chi(0,0)|_{\mu\to\mu-q}$ for $\{\alpha,\beta\} = \{1,-1\}$. The transverse spin response given by $(\chi^0)^{10}_{01}(p,\omega)$ cannot be simply expressed in terms of χ. Nonetheless, one can develop an expression analogous to Eq.A-2. First we integrate out the angular variables to find:

$$(\chi^0)^{10}_{01\mathbf{p}}(\omega) = \frac{-m}{\pi\lambda_T^2 p}\int_0^\infty d\tilde{k} n(\epsilon_{\tilde{k}1}) \log\left(\frac{z_- - \tilde{k}}{z_- + \tilde{k}}\right) + n(\epsilon_{\tilde{k}0}) \log\left(\frac{z_+ - \tilde{k}}{z_+ + \tilde{k}}\right) \qquad \text{(A-3)}$$

where $z_\pm = \frac{\omega+q}{2\sqrt{\epsilon_p k_B T}} \pm \frac{p\Lambda_T}{4\sqrt{\pi}}$ and $\tilde{k} = k\Lambda_T/4\sqrt{\pi}$. We use $\tilde{k}$ as an expansion parameter.

Rewriting the logarithm as an integral we get:

$$(\chi^0)^{10}_{01}(p,\omega) = -\frac{m}{2\pi\lambda_T^2 p}\left(\int_\infty^{z_-} dx I_1(k) - \int_\infty^{z_+} dx I_0(k) \right) \qquad \text{(A-4)}$$

where $I_{1/0}(k) = \int_{-\infty}^{\infty} dk \frac{1}{k-x} \frac{2k}{e^{k^2+\beta\lambda_{1/0}}-1}$, where $\lambda_1 = -\beta(\mu - q)$ and $\lambda_0 = -\beta\mu$. The analytic structure of the integral I has been extensively developed by Szépfalusy and Kondor [29], who show that the integral can be written as an asymptotic series for long wave-lengths. Retaining only the lowest order terms we find that the static response is:

$$(\chi^0)^{10}_{01}(0,0) = \frac{m}{4\pi\lambda_T}\frac{k_B T}{q}(g_{3/2}(e^{\beta(\mu-q)}) - g_{3/2}(e^{\beta\mu})) \qquad \text{(A-5)}$$

which is our desired result.

The non-interacting pair response is defined as:

$$(\Pi^0)^{\alpha\beta}_{\beta\alpha}(\mathbf{p},\omega) = \int \frac{d^3\mathbf{k}}{(2\pi)^3} \frac{n(\epsilon_{\mathbf{k},\alpha}) + n(\epsilon_{\mathbf{k}+\mathbf{p},\beta})}{\omega - (\epsilon_{\mathbf{k}+\mathbf{p}\beta} + \epsilon_{\mathbf{k}\alpha})} \quad \text{(A-6)}$$

The pair susceptibility for the scalar gas has been considered in [8]. The result to linear order in $k\Lambda_T$ is :

$$\Pi^0(\mathbf{p},0) = -\frac{m}{\pi\lambda_T}\left(g_{1/2}(e^{\beta\mu}) - \sqrt{|\pi/(\beta\mu)|}\right. \quad \text{(A-7)}$$
$$\left. + \frac{2i\pi}{p\Lambda_T}\log\left(\frac{(1+i)\frac{p\Lambda_T}{4\sqrt{\pi}} - \sqrt{\beta\mu}}{(1-i)\frac{p\Lambda_T}{4\sqrt{\pi}} - \sqrt{\beta\mu}}\right) + \frac{p\Lambda_T}{8}\right)$$

It is easy to show that $(\Pi^0)_{-1\ 1}^{\ 1-1}(0,0) = \Pi^0(0,0)|_{\mu\to\mu-q}$ and $(\Pi^0)^{00}_{00} = \Pi^0$.

Appendix B: Spin response in the RPA

The spin response in the RPA is given by solving for the polarization tensor defined in the main text. The interaction matrix $V^{\gamma\eta}_{\mu\nu}$ encompasses all direct and exchange diagrams and represents an process wherein in two particles with spin γ and η are destroyed to create two particles with spin μ and ν. Conservation of spin forces the constraint: $\gamma + \eta = \mu + \nu$. As there are 9 difference choices for the spins of the pairs of particles $|\psi_\gamma\psi_\eta\rangle$, V is a 9×9 matrix in this basis. Expressed below, from left to right and top to bottom $|\gamma\eta\rangle = |11\rangle, |10\rangle, |1-1\rangle, |01\rangle, |00\rangle, |0-1\rangle, |-11\rangle, |-10\rangle, |-1-1\rangle$.

$$V = \begin{pmatrix} 2(c_0+c_2) & 0 & 0 & 0 & c_0+c_2 & 0 & 0 & 0 & c_0-c_2 \\ 0 & 0 & 0 & c_0+c_2 & 0 & 0 & 0 & 2c_2 & 0 \\ 0 & 0 & 0 & 0 & 0 & 0 & c_0-c_2 & 0 & 0 \\ 0 & c_0+c_2 & 0 & 0 & 0 & 2c_2 & 0 & 0 & 0 \\ c_0+c_2 & 0 & 0 & 0 & 2c_0 & 0 & 0 & 0 & c_0+c_2 \\ 0 & 0 & 0 & 2c_2 & 0 & 0 & 0 & c_0+c_2 & 0 \\ 0 & 0 & c_0-c_2 & 0 & 0 & 0 & 0 & 0 & 0 \\ 0 & 2c_2 & 0 & 0 & 0 & c_0+c_2 & 0 & 0 & 0 \\ c_0-c_2 & 0 & 0 & 0 & c_0+c_2 & 0 & 0 & 0 & 2(c_0+c_2) \end{pmatrix} \quad \text{(B-1)}$$

From the full polarization tensor, one extracts the longituginal and transverse spin susceptibility on which our calculations are based.

We now turn to the details of the pair response calculation.

Appendix C: Pairing response in the RPA

The RPA pair response is calculated in a similar manner to the magnetic response. However since pairing only occurs in the $S_z = 0$ channel, it suffices to consider the following subsystem

$$\overleftrightarrow{\Pi} = \begin{pmatrix} \Pi_{-1\ 1}^{\ 1-1} & \Pi_{0\ 0}^{\ 1-1} & \Pi_{1-1}^{1\ 1-1} \\ \Pi_{1-1}^{0\ \ 0} & \Pi_{00}^{00} & \Pi_{-11}^{\ \ 00} \\ \Pi_{-11}^{-1\ 1} & \Pi_{\ 00}^{-1\ 1} & \Pi_{1-1}^{-1\ \ 1} \end{pmatrix}^{RPA} \quad \text{(C-1)}$$

which is related to the non-interacting response

$$(\overleftrightarrow{\Pi})^0 = \begin{pmatrix} (\Pi^0)_{-1\ 1}^{\ 1-1} & 0 & 0 \\ 0 & (\Pi^0)^{00}_{00} & 0 \\ 0 & 0 & (\Pi^0)^{-1\ \ 1}_{1-1} \end{pmatrix}$$

and the 3×3 interaction matrix

$$V = \begin{pmatrix} c_0 - c_2 & c_2 & 0 \\ c_2 & c_0 & c_2 \\ 0 & c_2 & c_0 - c_2 \end{pmatrix}$$

by the equation

$$(\Pi^{RPA})^{\gamma\eta}_{\alpha\beta} = (\Pi^0)^{\gamma\eta}_{\alpha\beta}\delta_{\alpha\eta}\delta_{\beta\gamma} + \sum_{\mu\nu}(\Pi^0)^{\gamma\eta}_{\eta\gamma}\mathbf{V}^{\gamma\eta}_{\mu\nu}(\Pi^{RPA})^{\mu\nu}_{\gamma\eta} \quad \text{(C-2)}$$

Two limiting cases are worth considering. The first is at $\mu = q$ for $q < 0$ when the non-interacting BEC transition occurs for the ± 1 atoms. At these values the non-interacting response function $\Pi_{-1\ 1}^{\ 1-1}$ diverges, and:

$$\Theta^{-1} \propto -c_0 + c_2 + (c_0 - 2c_2)(c_0 + c_2)\Pi^{00}_{00} \quad \text{(C-3)}$$

The second is at $\mu = 0$ which corresponds to the BEC transition for the 0 atoms. At this point non-interacting response function Π^{00}_{00} diverges and:

$$\Theta^{-1} \propto -c_0 + (c_0 - 2c_2)(c_0 + c_2)\Pi_{-1\ 1}^{\ 1-1} \quad \text{(C-4)}$$

Setting $\Theta^{-1} = 0$ in Eqs. (C-3, C-4) to zero yields the threshold value of c_2 at which paired states result for any q.

[1] Clarina de la Cruz *et al.* Nature, **453** 899-902 (2002); M. Kenzelmann *et al.* Science **321** (5896) (2008); A. J. Drew *et al.* Nature Materials, **8** 310-314 (2009); Y-A. Liao *et al.*, Nature **467** 567-569 (2010).

[2] J. Stenger, *et al.*, Nature **396** 345 (1998). L.E.Sadler, *et al.*, ibid., **443** (2006); D. M. Stamper-Kurn, *et al.*, Phys. Rev. Lett. **80**, 2027 (1998); J. Kronjäger, *et al.*, ibid. **105** 090402 (2010); M.Vengalattore, *et al.*, Phys. Rev. Lett., **100** 170403 (2008); D. S. Hall *et al.*, ibid., Phys. Rev. Lett. **81** 243 (1998).

[3] Tin-Lun Ho, Phys. Rev. Lett., **81** 742 (1998).

[4] T.Ohmi and K.Machida, J. Phys. Soc. Jpn., **67** 1822, (1998).

[5] Erich J. Mueller, Phys. Rev. A **69**, 033606 (2004).

[6] D. Podolsky, S. Chandrasekharan and A. Vishwanath, Phys. Rev. B **80** 214513 (2009). E. Demler and F. Zhou, Phys. Rev. Lett. **88** 163001 (2002); K. Murata, H. Saito and M. Ueda, Phys. Rev. A **75** 013607 (2007); A. Lamacraft, Phys. Rev. Lett.**98** 160404 (2007).

[7] S. Ashaab, J. Low Temp. Phys. **140** 51 (2005).

[8] E. J. Mueller and G. Baym, Phys. Rev. A **62** 053605 (2000).

[9] P. Nozières and D. Saint James, J. Phys (Paris) **43** (1982).

[10] F. Gerbier, A. Widera, S. Folling, O. Mandel and I. Bloch, Phys. Rev. A **73**, 041602(R) (2006).

[11] C.K. Law, H. Pu and N. P. Bigelow, Phys. Rev. Lett. **81**, 5257 (1998).

[12] E. J. Mueller, T-L. Ho, M. Ueda and G. Baym, Phys. Rev. A **74** 033612 (2006).

[13] S. Mukerjee, C. Xu and J.E. Moore, Phys. Rev. Lett. **97**, 120406 (2006).

[14] A. J. A. James and A. Lamacraft, arxiv:1009.0043.

[15] Kun Yang, eprint. arxiv: 0907.4739.

[16] Q. Gu and R. A. Klemm, Phys. Rev. A. **68** 031604 (R).

[17] K. Kis-Szabó, P. Szépfalusy and G. Szirmai, Phys. Rev. A **72** 023617 (2005).

[18] S. Pilati *et al.* Phys. Rev. A **74** 043621 (2006).

[19] M. Holzmann, W. Krauth and M. Naraschewski, Phys. Rev. A **59** 2956 (1999).

[20] J. W. Negele and H. Orland, *Quantum Many-Particle Systems* Westview Press, Boulder Colorado 1998.

[21] P. Szépfalusy and G. Szirmai, Phys. Rev. A **65** 043602 (2002).

[22] E. Stoner, Phil. Mag. **15** 1018 (1933).

[23] D. J. Papoular, G. V. Shlyapnikov, and J. Dalibard, Phys. Rev. A **81** 041603 (R) (2010).

[24] A. Imambekov, M. Lukin and E. Demler, Phys. Rev. A **68** 063602 (2003).

[25] Mukund Vengalattore, Private Communications.

[26] James P. Burke, PhD Thesis (1999).

[27] I. Carusotto and E. Mueller, J. Phys. B **37** S115 (2004).

[28] M. Greiner, *et al.*, Phys. Rev. Lett. **94** 110401 (2005).

[29] P. Szépfalusy and I. Kondor, Ann. Phys. **82** 1 (1974).